

NACA RM E53L11b

TECH LIBRARY KAFB, NM
0143272

NACA

RESEARCH MEMORANDUM

AERODYNAMIC CHARACTERISTICS OF TWO FLAT-BOTTOMED

BODIES AT MACH NUMBER OF 3.12

By John R. Jack and Barry Moskowitz

Lewis Flight Propulsion Laboratory
Cleveland, Ohio

Classification cancelled (or changed to) UNCLASSIFIED
By authority of: NASA Tech Rep Announcement # 123
(OFFICER AUTHORIZED TO CHANGE)

By 7 Jan 58
NAME AND

W. M. B.
GRADE OF OFFICER MAKING CHANGE)

20 Mar 61
DATE

NATIONAL ADVISORY COMMITTEE
FOR AERONAUTICS

WASHINGTON

April 2, 1954



0143272

NACA RM E53L11b

~~CONFIDENTIAL~~

NATIONAL ADVISORY COMMITTEE FOR AERONAUTICS

RESEARCH MEMORANDUM

AERODYNAMIC CHARACTERISTICS OF TWO FLAT-BOTTOMED

BODIES AT MACH NUMBER OF 3.12

By John R. Jack and Barry Moskowitz

SUMMARY

The aerodynamic characteristics of two flat-bottomed bodies having a semicircular and a semielliptical cross section have been determined at a Mach number of 3.12 for a range of angles of attack from -10° to 10° and for Reynolds numbers of 8×10^6 and 14×10^6 (based on model length).

A comparison of the flat-bottomed body characteristics with those previously determined for a corresponding cone-cylinder body of revolution shows that significant increases in lift and lift-drag ratio are obtained with a flat bottom. Additional improvement in lift and lift-drag ratio was achieved at positive angles of attack by expanding the plan form in the spanwise direction.

INTRODUCTION

Possible variations in missile body designs to achieve greater lift and better over-all lift-drag ratios are of considerable interest. Recent experimental investigations (see refs. 1 and 2) indicate that the lift-drag ratio of a blunt-based body of revolution may be increased both by increasing the afterbody length and by increasing the nose fineness ratio. Sanger (ref. 3) first proposed the use of flat-bottomed bodies to increase the lift and lift-drag ratio of missile configurations. Results of two investigations of flat-bottomed bodies at a Mach number of 6.9 are presented in reference 4, and the aforementioned possibilities of flat-bottomed bodies have been verified at hypersonic speeds. The question immediately arises, however, as to their effectiveness and behavior in the supersonic speed range.

This report presents the results of an investigation in the NACA Lewis 1- by 1-foot supersonic wind tunnel of two flat-bottomed bodies to determine their aerodynamic characteristics at a Mach number of 3.12. These characteristics are compared with those previously determined (ref. 5) for a cone-cylinder body of revolution to establish the effectiveness of flat-bottomed bodies at supersonic velocities.

~~CONFIDENTIAL~~~~Handwritten signature/initials~~

3204

CK-1

APPARATUS AND PROCEDURE

Wind Tunnel

The tests were conducted in the Lewis 1- by 1-foot supersonic wind tunnel which is a continuous-flow, nonreturn, variable pressure wind tunnel operating at a Mach number of 3.12. Inlet pressures may be varied from 6 to 52 pounds per square inch at a stagnation temperature of approximately 60° F, giving a free-stream Reynolds number variation of 1 to 8×10^6 per foot. The specific humidity of the inlet air was sufficiently low (about 2×10^{-5} pound water per pound dry air) to minimize the effects of condensation.

Models

The pertinent dimensions of the test configurations are shown in figure 1. The basic model for comparison (model A of fig. 1) is a cone-cylinder body of revolution 12 diameters long having a 4° 46' conical half-angle and a nose 6 diameters long. Models B and C have basic dimensions identical to model A; however, their cross-sectional areas are semicircular and semielliptical, respectively. The cross-sectional area of the semielliptical body is twice that of the semicircular body and equal to that of the cone-cylinder body of revolution. In choosing the cross-sectional shapes no consideration was given to the utilization of the enclosed volume of the flat-bottomed bodies for a pay load.

Measurements

Forces were obtained for an angle of attack range of -10° to 10° by means of an internally mounted three-component strain-gage balance. Unfortunately, however, the sensitivity of the balance system was such that the axial loads for Reynolds number $Re = 2 \times 10^6$ (based on body length) were generally of the same order of magnitude as the accuracy of the balance system; hence the data for $Re = 2 \times 10^6$ are not presented. The estimated errors in the experimentally determined force coefficients (based on frontal area) are believed to be as follows for $Re = 14 \times 10^6$:

Force coefficient	Estimated error
Drag	± 0.01
Lift	± 0.03
Moment	± 0.01

Model base pressures were obtained by means of an orifice located in the balance chamber just inside the base of the model. These base pressures were used to correct the measured axial forces to the condition of zero base drag; hence, all force coefficients apply to the forebody (body forward of the base).

RESULTS AND DISCUSSION

The variation of the experimental drag and lift coefficients (based on frontal area) and the lift-drag ratio for models A, B, and C are presented in figures 2, 3, and 4, respectively, for Reynolds numbers of 8×10^6 and 14×10^6 . As indicated in figures 3, 4, and 5, the effect of changing the Reynolds number from 8×10^6 to 14×10^6 is quite small; however, on the basis of past experience and the experimental data obtained at $Re = 2 \times 10^6$, the drag is probably affected considerably at the lower Reynolds numbers (see, for example, ref. 5 from which the cone-cylinder data were obtained). Both flat-bottomed bodies have drag and lift coefficients higher than those for the cone-cylinder body of revolution at corresponding angles of attack. The drag coefficients are nearly symmetrical with respect to angle of attack and the lift coefficients are nearly antisymmetrical. A comparison of the lift-drag ratios of the three models shows that in spite of experiencing the largest drag, the semielliptical model has the largest lift-drag ratio at positive angles of attack. The combined deviations from a body of revolution incorporated in model C, that is, flattening the bottom and increasing the width of the plan form, netted a maximum lift-drag ratio at 6° angle of attack 1.85 times that of the cone-cylinder body of revolution at this angle of attack. However, for a given lift coefficient, the lift-drag ratios are approximately equal. At negative angles of attack, model B (semicircular) appears to be maximizing at a larger value than model C (semielliptical) and at a higher angle of attack.

The fact that the semielliptical body possesses the highest maximum lift-drag ratio testifies to the desirability of expanding the plan form of the flat-bottomed bodies in the spanwise direction. It must be borne in mind, however, that expanding the plan form in the spanwise direction has increased both the aspect ratio of the cross section and also the aspect ratio of the plan form, so that the parameter affecting the lift-drag ratio has not been definitely established.

The variation of the center of pressure locations with angle of attack is presented in figure 5. Here again the effect of Reynolds number is not noticeable. Both flat-bottomed bodies, however, have approximately the same center of pressure location over the angle of attack range investigated.

3204

CK-1 back

~~CONFIDENTIAL~~

CONCLUSIONS

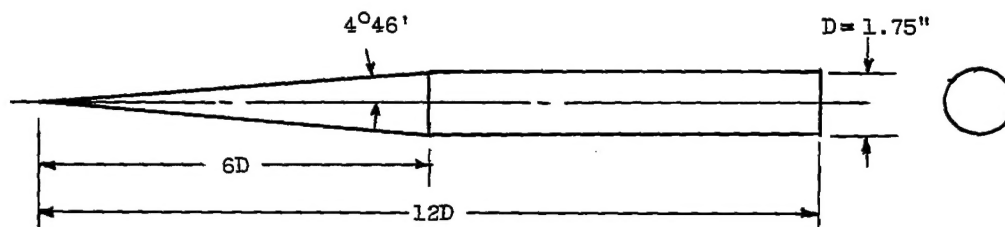
The aerodynamic characteristics of a semicircular and a semielliptical cone-cylinder body have been obtained at a free-stream Mach number of 3.12 and for Reynolds numbers of 8×10^6 and 14×10^6 . An analysis of the results may be summarized as follows:

1. Flat-bottomed bodies provide large gains in both lift and lift-drag ratio as compared with a corresponding body of revolution.
2. An additional increase in lift and lift-drag ratio was obtained at positive angles of attack by expanding the plan form in the spanwise direction.
3. With respect to angle of attack, the drag coefficients are nearly symmetrical and the lift coefficients are nearly antisymmetrical.
4. Changing the Reynolds number from 8×10^6 to 14×10^6 had little effect on the aerodynamic characteristics.

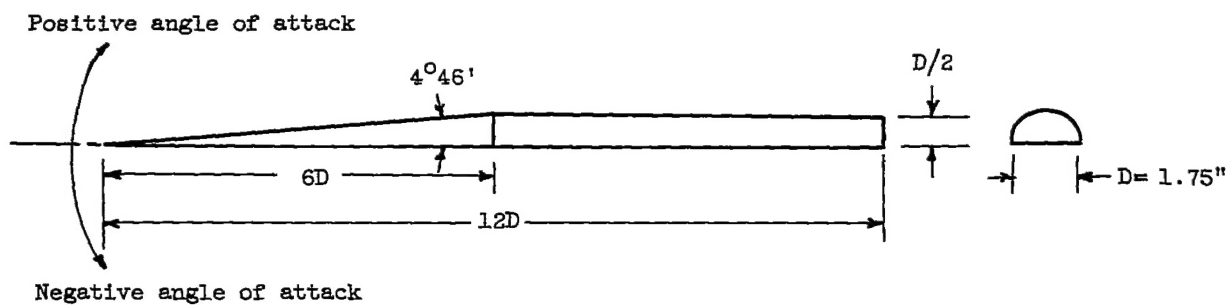
Lewis Flight Propulsion Laboratory
National Advisory Committee for Aeronautics
Cleveland, Ohio, December 16, 1953

REFERENCES

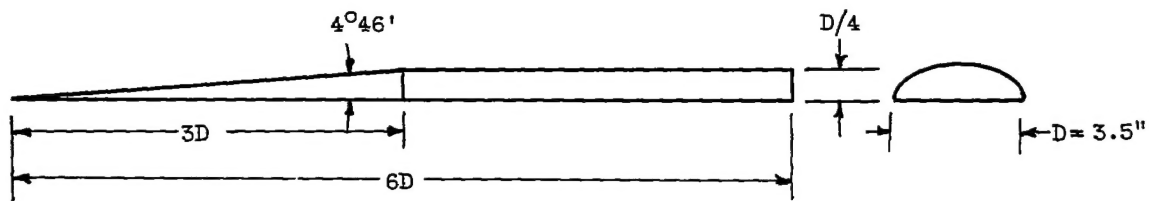
1. Cooper, Ralph D., and Robinson, Raymond A.: An Investigation of the Aerodynamic Characteristics of a Series of Cone-Cylinder Configurations at a Mach Number of 6.86. NACA RM L51J09, 1951.
2. Jack, John R., and Moskowitz, Barry: Aerodynamics of Slender Bodies at Mach Number of 3.12 and Reynolds Numbers from 2×10^6 to 15×10^6 . IV - Aerodynamic Characteristics of Series of Four Bodies Having Near Parabolic Noses and Cylindrical Afterbodies. NACA RM E53J27, 1954.
3. Sanger, E., and Bret, J. (M. Hamermesh, trans.): A Rocket Drive for Long Range Bombers. Trans. CGD-32, Tech. Info. Branch, BuAer, Navy Dept., Aug., 1944.
4. McLellan, Charles H.: Exploratory Wind-Tunnel Investigation of Wings and Bodies at $M = 6.9$. Jour. Aero. Sci., vol. 18, no. 10, Oct. 1951, pp. 641-648.
5. Jack, John R.: Aerodynamics of Slender Bodies at Mach Number of 3.12 and Reynolds Numbers from 2×10^6 to 15×10^6 . III - Boundary Layer and Force Measurements on a Slender Cone-Cylinder Body of Revolution. NACA RM E53B03, 1953.



(a) Model A; circular cone-cylinder body (ref. 5).



(b) Model B; semicircular cone-cylinder body.



(c) Model C; semielliptical cone-cylinder body.

Figure 1. - Pertinent dimensions of test configurations.

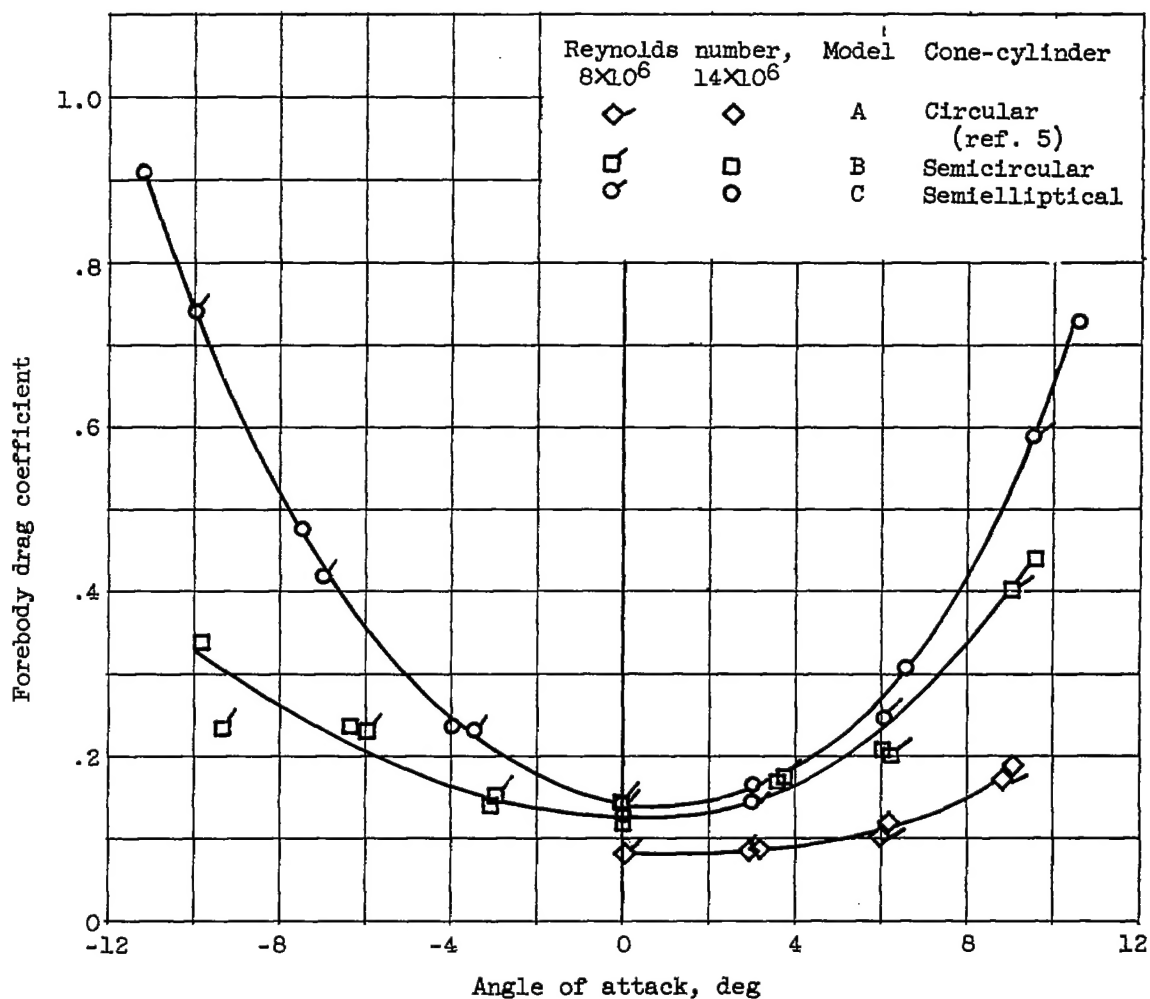
~~CONFIDENTIAL~~

Figure 2. - Variation with angle of attack of forebody drag coefficient for Reynolds numbers of 8×10^6 and 14×10^6 .

~~CONFIDENTIAL~~

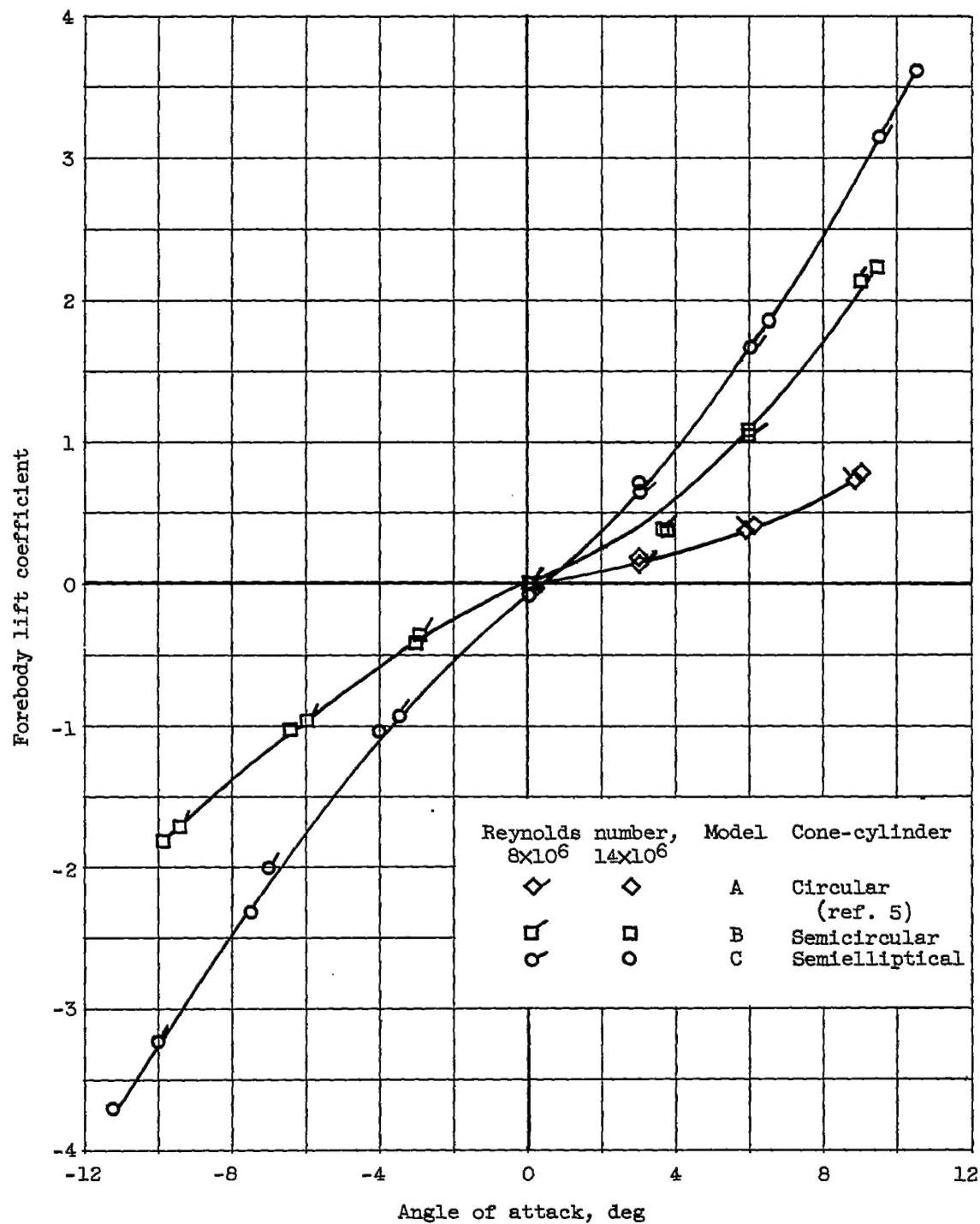


Figure 3. - Variation with angle of attack of forebody lift coefficient for Reynolds numbers of 8×10^6 and 14×10^6 .

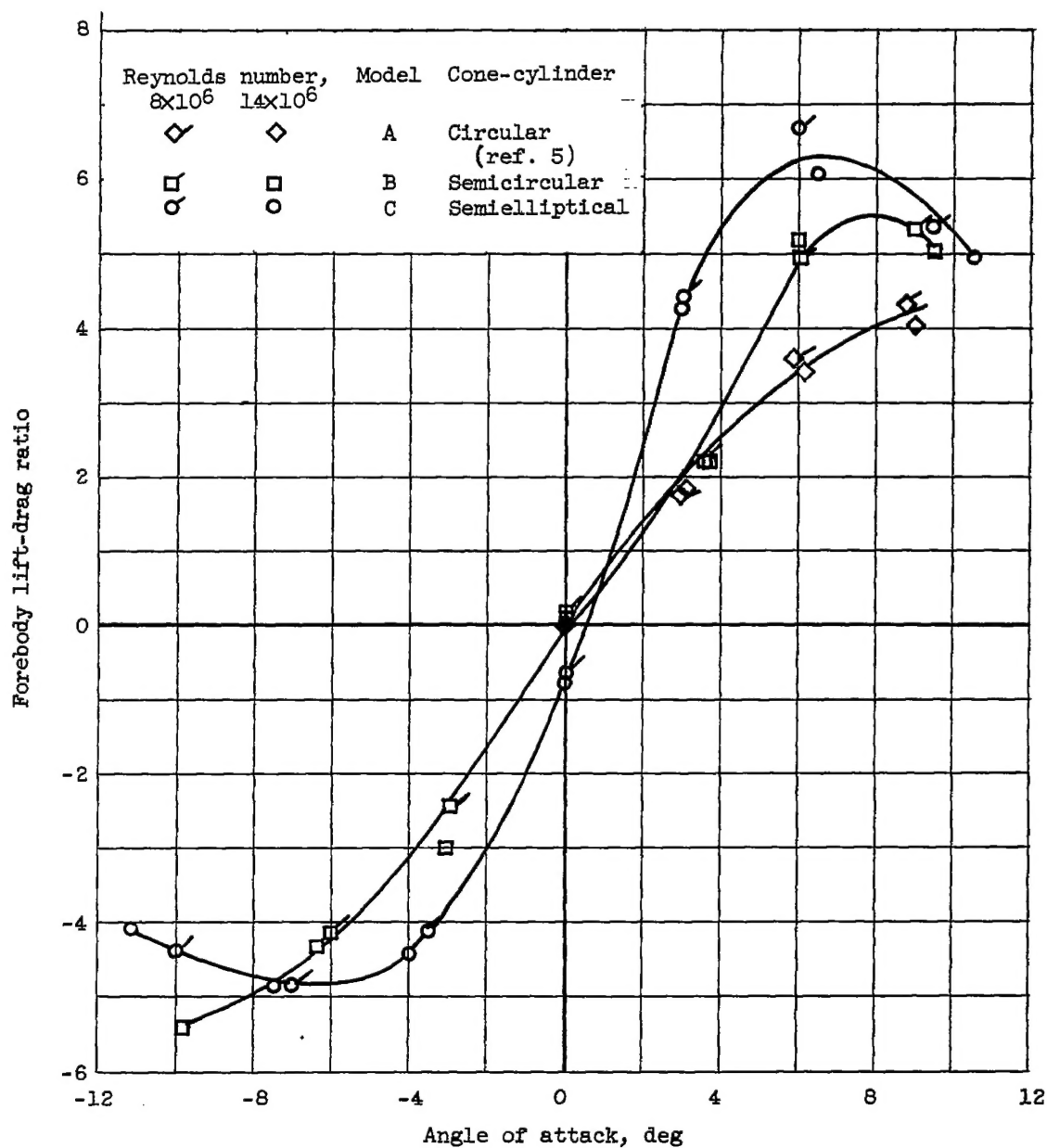


Figure 4. - Variation with angle of attack of forebody lift-drag ratio for Reynolds numbers of 8×10^6 and 14×10^6 .

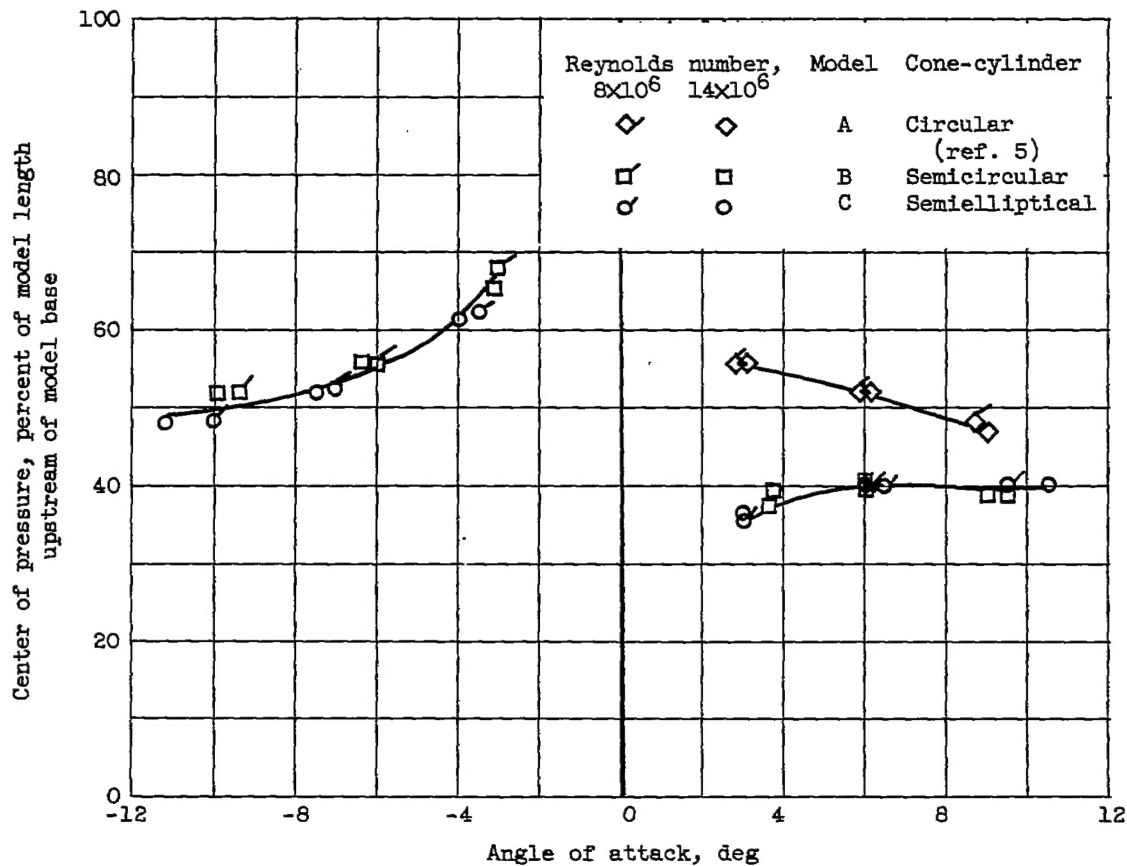


Figure 5. - Variation with angle of attack of center of pressure (percent of model length upstream of model base) for Reynolds numbers of 8×10^6 and 14×10^6 .